The Journal of Infectious Diseases

MAJOR ARTICLE

Plasma Proteomics Reveals Distinct Signatures in Occult and Microfilaremic *Loa loa* Infections

Clemens Dierks,[1,2,a] Pinkus Tober-Lau,[2,a] Luzia Veletzky,[3,4,a] Ziyue Wang,[1] Boris Zühlke,[1] Daniela Ludwig,[5] Agathe Niewienda,[5] Anja Freiwald,[5] Lara Bardtke,[2] Paolo Kroneberg,[2] Daniel Stelzl,[4,6] Jennifer Hergeth,[4] Rella Zoleko Manego,[4,7,8] Ghyslain Mombo-Ngoma,[4,9] Selidji Todagbe Agnandji,[4,10,11] Ayola Akim Adegnika,[4,11,12] Michael Mülleder,[5] Michael Ramharter,[4,7,8,b] Markus Ralser,[1,13,14,b] and Florian Kurth[2,4,7,b]

[1]Institute of Biochemistry, Charité–Universitätsmedizin Berlin, Corporate Member of Freie Universität Berlin and Humboldt Universität zu Berlin, Berlin, Germany; [2]Department of Infectious Diseases and Critical Care Medicine, Charité–Universitätsmedizin Berlin, Corporate Member of Freie Universität Berlin and Humboldt Universität zu Berlin, Berlin, Germany; [3]Division of Infectious Diseases and Tropical Medicine, Department of Medicine I, Medical University of Vienna, Vienna, Austria; [4]Centre de Recherches Médicales de Lambaréné, Lambaréné, Gabon; [5]Core Facility High Throughput Mass Spectrometry, Charité—Universitätsmedizin Berlin, Corporate Member of Freie Universität Berlin and Humboldt Universität zu Berlin, Berlin, Germany; [6]Department of Urology, University Medical Center Hamburg-Eppendorf, Hamburg, Germany; [7]Center for Tropical Medicine, Bernhard Nocht Institute for Tropical Medicine and I. Department of Medicine University Medical Center Hamburg-Eppendorf, Hamburg, Germany; [8]German Center for Infection Research, Partner Site Hamburg-Lübeck-Borstel-Riems, Hamburg, Germany; [9]Section of Implementation Research, Bernhard Nocht Institute for Tropical Medicine, Hamburg, Germany; [10]Institute for Medical Microbiology, University of Münster, Münster, Germany; [11]Institute for Tropical Medicine, University of Tübingen, Tübingen, Germany; [12]German Center for Infection Research, Partner Site Tübingen, Tübingen, Germany; [13]Max Planck Institute for Molecular Genetics, Berlin, Germany; and [14]Centre for Human Genetics, Nuffield Department of Medicine, University of Oxford, Oxford, United Kingdom

Background. Loiasis, caused by the filarial nematode *Loa loa*, imposes a significant disease burden in endemic regions in West and Central Africa. Manifestations include adult worms in soft tissue (e.g., the conjunctiva of the eye) and microfilaria in peripheral blood, with clinical presentations ranging from asymptomatic infections to life-threatening organ involvement. Diagnosis remains challenging due to variable microfilaria counts, frequent amicrofilaremic occult infections, and unreliable serological tests. The untargeted plasma proteome reflects broad (patho-)physiological responses, providing valuable insights into the host and disease.

Methods. Applying high-throughput plasma proteomics, we investigated the host responses of 274 patients with different *L. loa* disease states, including occult loiasis (n = 148), microfilaremia (n = 42), or both (n = 84), compared to 136 *L. loa*–negative controls. Differentially abundant proteins between *L. loa*–infected individuals and negative controls were validated using targeted proteomics.

Results. Five proteins (IGHG3, IGHG4, ACTBL2, LCP1, and IGLV9-49) were elevated in infected individuals compared to healthy controls. IGHG3, IGHG4, ACTB, and LCP1 increased from *L. loa* negative over individuals with history of eye worm migration to microfilaremic patients, indicating a comparatively pronounced proteomic host response to microfilaria in the blood. Sixty-three proteins differed depending on self-reported symptoms. The proteomic signatures enabled accurate classification of individuals with occult loiasis (area under the receiver operating characteristic curve [AUROC] = 0.73) and microfilaremia (AUROC = 0.84) by a random forest machine learning model.

Conclusions. Overall, infection with *Loa loa* alters the host plasma proteome, exhibiting distinct host responses in different infection states and allowing for molecular disease classification of this highly neglected parasitic disease.

Keywords. plasma proteomics; neglected tropical disease; *Loa loa*; mass spectrometry; infectious disease.

Loiasis is a parasitic disease caused by the filarial nematode *Loa loa*, which is transmitted by the blood-feeding *Chrysops* fly endemic to the tropical rain forests of Central and West Africa, where >20 million people are estimated to be infected [1]. Despite its high regional prevalence, it is a highly neglected disease not yet even figuring on the World Health Organization's (WHO) list of neglected tropical diseases (NTDs) [2–4]. This is likely because, until recently, it has been regarded as a relatively benign condition compared to lymphatic filariasis or onchocerciasis, which are both recognized as NTDs by WHO [1–4]. However, more recent data indicate a considerable burden of disease and excess mortality in affected communities [1, 2, 4–6].

The complex clinical manifestation of *L. loa* infection can range from asymptomatic infection, pruritus, and the pathognomonic

Received 25 November 2024; editorial decision 23 June 2025; accepted 25 June 2025; published online 17 July 2025

[a]C. D., P. T.-L., and L. V. contributed equally to this work.

[b]M. Ram., M. Ral., and F. K. contributed equally to this work.

Correspondence: Florian Kurth, MD, Department of Infectious Diseases and Critical Care Medicine, Charité–Universitätsmedizin Berlin, Augustenburger Platz 1, Berlin 13353, Germany (florian.kurth@charite.de).

The Journal of Infectious Diseases® 2025;232:e383–92

https://doi.org/10.1093/infdis/jiaf344

Calabar swelling, a localized transient nonpitting edema usually above bony prominences, to potentially life-threatening organ manifestations including endomyocardial fibrosis, kidney injury, and encephalopathy [1, 7–10]. Approximately 80% of infected patients eventually observe the adult worm migrating through the conjunctiva of the eye, earning it the name "African eye worm" [1].

Diagnosis of *L. loa* is typically established by (self-) reported history of an eye worm episode or through the identification of circulating microfilariae in the blood by light microscopy. Detectable microfilaremia in peripheral blood shows diurnal periodicity, matching *Chrysops*' blood-feeding pattern and complicating diagnosis. Furthermore, presence of blood microfilariae differs considerably between infected individuals, ranging from hypermicrofilaremia of >30 000 microfilariae (mf)/mL to complete amicrofilaremia [1]. Some of the patients with this latter condition, often referred to as "occult loiasis," seem to mount an effective immune response to the parasite, possibly aided by genetic factors that modify susceptibility to infection and symptom expression [1, 10–12].

Newer diagnostic approaches for loiasis include quantitative polymerase chain reaction (PCR), which, like microscopy, demonstrates high specificity but only moderate sensitivity, especially in patients with low microfilaremia, and serological assays, which are highly cross-reactive with other helminth infections and can exhibit low sensitivity in individuals with high microfilarial counts [12]. However, there are currently no biomarker tests available that inform about the state of disease. The standardized RAPLOA (Rapid Assessment Procedure for Loiasis) questionnaire thus remains the diagnostic standard for occult loiasis [13, 14].

In this study, we pursued an approach complementary to diagnostics, aiming to identify host signatures that capture microfilaremic and occult loiasis by using plasma proteomics. As the function of many proteins is mapped, such signatures can help to understand pathophysiological and immunological mechanisms of infections [15, 16] and contribute to improving the diagnosis and management of this neglected infectious disease.

MATERIALS AND METHODS

Patient Cohort and Clinical Laboratory Diagnostics

Data and samples were collected as part of a study investigating the burden of *L. loa*–associated disease in a highly endemic region in central Gabon [2, 8, 12]. In brief, between 2017 and 2018, a community survey was performed, using a standardized questionnaire for demographic data and known *L. loa*–associated symptoms, including history of eye worm migration by the RAPLOA questionnaire [13]. Venous blood samples for parasite and hematological diagnostics were collected in ethylenediaminetetraacetic acid tubes between 10 AM and 3 PM. Microfilaria diagnostics were performed by light microscopy of Giemsa-stained thick blood smears or 1 mL lysed and centrifuged whole blood using an Olympus CH30 or Nikon Eclipse E200 microscope. For microscopically negative samples, PCR from 500 µL whole blood was performed (Supplementary Methods) [17, 18]. Participants were subsequently classified as *L. loa* negative (LN), microfilaria positive (MF), eye worm positive (EW), or eye worm and microfilaria positive (EWMF). Participants younger than 18 years, with known pregnancy [19], or with *Mansonella perstans* or *Plasmodium* spp. infections were excluded. Additionally, individuals with eosinophilia >500 cells/µL were excluded from the group of *L. loa*–negative controls in order to reduce the probability of undetected helminth infections [20]. Ethics approval was provided by the local institutional review board (Comité d'Éthique Institutionnel du Centre de Recherches Médicales de Lambaréné; IORG0007336/IRB00008812; CEI-011/2017), and all participants or their legal guardians provided written informed consent prior to all study procedures [19].

Sample Preparation, Liquid Chromatography, and Mass Spectrometry

Sample preparation was performed using a semi-automated in-solution digestion with trypsin, followed by cleanup using C_{18} solid phase extraction [21]. Samples were analyzed using an Agilent 1290 Infinity II liquid chromatography (LC) system with a 5-minute gradient, coupled to a timsTOF HT mass spectrometer (Bruker Daltonics) operating in diaPASEF acquisition mode, as previously described [15, 16, 21]. Validation measurements were performed with high-resolution multiple reaction monitoring (hrMRM) on an M-Class microflow LC system (Waters) coupled to a ZenoTOF 7600 mass spectrometer (Sciex). Full technical details are provided in the Supplementary Methods.

Data Processing and Statistical Data Analysis

For discovery proteomics, raw mass spectrometry (MS) data were processed with DIA-NN (v1.8.1; https://github.com/vdemichev/DiaNN) as previously described [22]. Peptide data was $\log_2$ transformed and missing values were imputed using the k-nearest-neighbors algorithm (*scikit-learn* v1.2.2) [23]. Peptide quantities were summarized to protein groups with the *MaxLFQ* algorithm as implemented in QuantUMS [24]. The hrMRM data were processed using *Skyline* (v23.1.0.268). No blinding was performed during peak integration. The quantity of each peptide was calculated by the summation of peak areas of each selected fragment of a peptide. Statistical data analysis was conducted using Python (v3.11), R (v4.3.3), and JMP Pro 17 (SAS Institute) software. The Quarto and R Markdown files that define and describe the analysis are available on GitHub (https://github.com/ClemensDie/loa_proteome).

The coefficient of variation (CV) was calculated for each protein by dividing the standard deviation (square root of variance) by the mean (average abundance), expressed as percentage.

Since the high-abundant plasma proteome is influenced by age and sex [25], with greatest changes to the proteome at age 34 and 60 years [26], individuals were categorized as

<34, 34–60 years, or >60 years of age, and balancing for age group and sex was performed using propensity score matching with the R *matchit* package. For validation experiments, *L. loa*–infected samples were randomly selected and corresponding *L. loa*–negative samples were matched for sex and age. Peptides with highest fold changes and significant differential expression were selected.

Differential expression analysis was performed with R's *limma* package. *P* values were adjusted using the Benjamini-Hochberg procedure and were considered significant when <.05. Statistical trend analysis was performed using Jonckheere-Terpstra tests (*clinfun* R package). The χ^2 test was employed to examine the statistical differences between nominal variables and Mann-Whitney *U* test for statistical group comparisons of hrMRM data (both *scipy*). Spearman rho was used to obtain correlation coefficients and linear regression models were fitted using *numpy* (*statsmodels*). To select the proteomic features that contain the most information, a random forest classifier was trained using the *scikit-learn* library (all Python). Additional details are provided in the Supplementary Methods.

RESULTS

Cohort Description and Sample Inclusion

Plasma samples were collected from 873 individuals living in central Gabon, including 623 with *L. loa* infection (INF) and 250 *L. loa*–negative controls (LN). Exclusion of samples due to low data quality (INF: n = 24; LN: n = 4), age <18 years (INF: n = 33; LN: n = 11), pregnancy (INF: n = 2; LN: n = 4), coinfection with *Plasmodium* spp. (INF: n = 68), *Mansonella* spp. (INF: n = 172), or both (INF: n = 50), and eosinophilia >500 cells/μL in *L. loa*–negative controls (n = 95) resulted in 274 INF and 136 LN controls included in this analysis. Out of the 274 INF, 42 (15.3%) had only detectable microfilaremia but no reported eye worm (MF), 148 (54.0%) had occult loiasis with history of eye worm migration (EW), and 84 (30.7%) had history of both eye worm migration and microfilaremia (EWMF) (Figure 1*A*). Age was similar between INF and LN individuals (median, 50 [interquartile range {IQR}, 38–62] years vs 48 [IQR, 31–59] years; $P = .09$), as was sex distribution (women: 161/274 [58.8%] vs 75/136 [55.2%], $P = .49$). Within the INF group, the proportion of women to men was higher among EW individuals (107/148 [72.3%], $P < .001$), lower among MF (12/42 [28.6%], $P < .001$), and similar among EWMF (42/84 [50.0%], $P = 1.0$). Detailed cohort characteristics are provided in Table 1.

Protein Profiling and Analytical Precision

The technical variation of protein abundances, measured in pooled samples, had a median CV of 17.16%, indicating the reproducibility of the measurement process itself. In contrast, the biological variation of protein abundances in study samples showed a median CV of 33.08%, reflecting the inherent biological variability across individual samples. Across all samples, a total of 273 high-abundance proteins and protein groups were consistently measured (Supplementary Figure 1, Supplementary Table 1, Supplementary Methods). These span over functional groups with clinical importance for their variation, with the highest biological response in immunoglobulins (n = 36, median CV: 49.41%). Compared to observations in general population studies [25], proteins involved in coagulation (n = 35 [25.31%]), acute phase response (n = 39 [26.33%]), the complement system (n = 16 [29.45%]), and lipid metabolism (n = 25 [32.87%]) showed a high diversity between individuals. The impact of age and sex on protein abundance between LN and INF groups was negligible (Supplementary Figures 2 and 3). Functional annotations for every protein measured are provided in Supplementary Table 2.

Proteomic Alterations in Different *L. loa* Disease States

When comparing age- and sex-matched LN to INF, we identified 5 plasma proteins that were significantly elevated in the INF group: immunoglobulin heavy constant gamma chain 3 and 4 (IGHG3 and IGHG4, respectively), beta-actin–like protein 2 (ACTBL2), plastin-2 (LCP1), and immunoglobulin lambda variable 9-49 (IGLV9-49) (Figure 1*B*, Supplementary Tables 3 and 4). To validate these findings, we established an independent targeted high-resolution multiple reaction monitoring (hrMRM) proteomic assay for these 5 proteins. We then quantified these proteins in randomly selected 10 INF and 10 matched LN samples (Supplementary Table 5). All 5 proteins showed higher abundance in INF, although IGLV9-49 did not achieve statistical significance in the validation (Supplementary Figure 4).

Investigating whether different *L. loa* disease states were reflected in the proteome, we found significantly higher levels of IGHG4 and beta-actin (ACTB) in MF compared to EW patients (Supplementary Figure 5*A*). Similarly, EWMF patients had higher levels of IGHG4 and profilin 1 (PFN1) than EW only (Supplementary Figure 5*B*). Yet, there were no significant differences between MF and EWMF groups (Supplementary Figure 5*C*). We observed an increasing trend in protein abundance from LN over EW to EWMF/MF in 4 proteins associated with *L. loa* infection states (Figure 1*C*). Since there were no differences between groups with microfilaremia, we investigated protein expression in MF + EWMF combined and EW versus LN (Supplementary Figures 5*D* and 5*E*). Protein regulation mostly correlated in both comparisons (lower left and upper right boxes in Figure 1*D*). However, higher levels of IGHG4, PFN1, ACTB, and S100A9 were observed in groups with microfilaremia (MF and EWMF), as well as greater abundance of sex hormone–binding globulin (SHBG) and fetuin B (FETUB) in the EW group. Details are provided in Supplementary Table 3.

We detected significant correlations between abundances of 19 proteins and microfilariae count (−0.22 to 0.37), including IGHG3, thyroxine-binding globulin (SERPINA7), immunoglobulin heavy constant delta, and LCP1 (Figure 1*E*). Notably, proteins

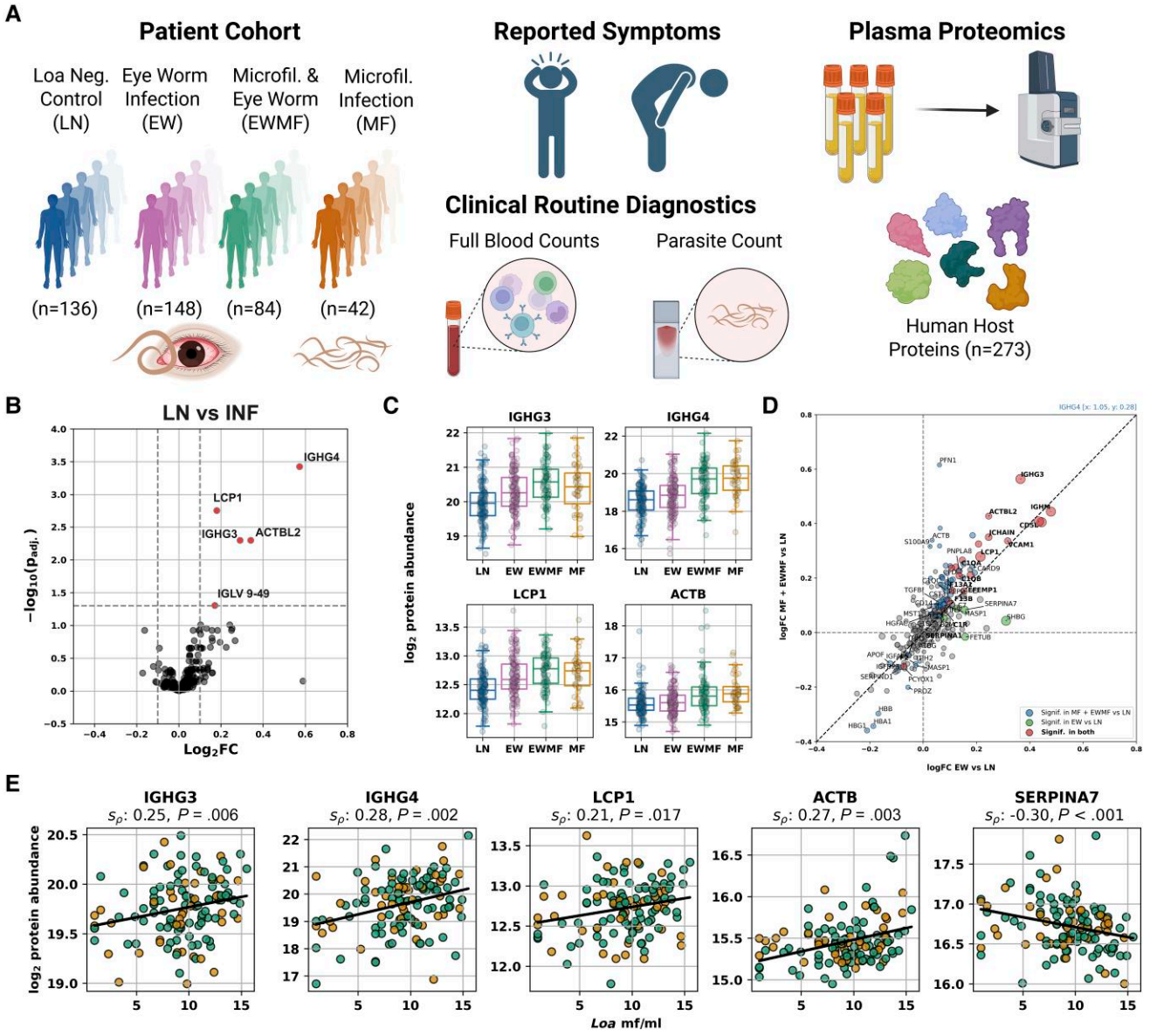

Figure 1. The human host plasma proteome response to *Loa loa* infection. *A*, Schematic overview of the study design to investigate the human host response to *L. loa* in patients with microfilaremia (MF) and/or history of eye worm migration (EW) and its interplay with reported symptoms and clinical routine diagnostics. *B*, Volcano plot depicting the contrast between *L. loa*–negative controls (LN) and all *L. loa*–infected cases (INF). *C*, Boxplots depicting abundances for 4 of the most prominent proteomic markers stratified by groups showing the difference between LN, patients with EW, patients with MF, and those with eye worm and microfilaremia (EWMF). Each scatter represents an individual patient sample. *D*, Scatter plot of $\log_2$ fold change (FC) for EW only and MF + EWMF combined vs LN. Size of scatter corresponds to statistical significance. Regulated proteins are color coded with red corresponding to the 21 proteins significant in both contrasts, blue corresponding to the 55 proteins significant only in the contrast MF + EWMF vs LN, and green corresponding to the 5 proteins significant only in the contrast EW vs LN. Scatters are labeled with gene symbols (abbreviated gene names). Those proteins found significant in both contrasts are highlighted with bold letters. For visualization purposes, IGHG4 and its regulation (in parentheses) was excluded from the scatterplot and displayed separately. *E*, Correlations between protein abundance and microfilariae counts (mf) for proteins with strongest correlation. Microfilariae counts were $\log_2$ transformed to show linear relationships. Spearman correlation coefficient and the respective *P* value are shown. Panel A was created with biorender.com.

that had highest correlations with the *L. loa* microfilarial count, such as PFN1 (0.37; log fold change: 0.62) and IGHG4 (0.25; 1.08), showed the strongest regulation in microfilarial infection (MF and EWMF; Figure 1*D*). Correlating the proteomic measurements with routine diagnostic markers, we found strong positive correlations for LCP1 (0.45) and IGHG4 (0.38) with absolute eosinophil counts, while IGHG3 (−0.38), IGHM (−0.36), C1q subunits (−0.28 to −0.35), and CD5L (−0.31) showed moderate negative and transthyretin (TTR) moderate positive correlations with absolute basophil counts (Supplementary Figure 6).

Identifying Symptom-Dependent Signatures in the Proteome

Occult (i.e., amicrofilariemic) loiasis has been associated with a higher symptom load compared to microfilaremic loiasis [8].

Table 1. Cohort Characteristics

Parameter	LN (n = 136)	INF (n = 274)	EW (n = 148)	EWMF (n = 84)	MF (n = 42)
Age, y	48 (31–59)	50 (38–62)	48 (35–62)	53 (42–62)	53 (41–64)
Female sex, no./No. (%)	75/136 (55.2%)	113/274 (41.2%)	107/148 (72.3%)	42/84 (50.0%)	12/42 (28.6%)
Loa loa count, mf/mL	0 (0–0)	0 (0–600)	0 (0–0)	825 (213–3738)	650 (138–4863)
Symptoms, no./No. (%)					
Arthralgia	35/135 (25.9%)	117/272 (43.0%)	61/146 (41.8%)	42/84 (50.0%)	14/42 (33.3%)
Myalgia	28/135 (20.7%)	89/272 (32.7%)	52/147 (35.4%)	27/83 (32.5%)	10/42 (23.8%)
Urticaria	36/136 (26.5%)	114/265 (43%)	70/143 (49.0%)	34/81 (42.0%)	10/41 (24.4%)
Pruritus	59/136 (43.4%)	123/274 (44.9%)	72/148 (48.6%)	35/84 (41.7%)	16/42 (38.1%)
Swelling	41/122 (33.6%)	127/247 (51.4%)	63/130 (48.5%)	48/78 (61.5%)	16/39 (41.0%)
Fatigue and headache	70/135 (51.9%)	184/270 (68.1%)	111/146 (76.0%)	53/83 (63.9%)	20/41 (48.8%)
Paresthesia and paralysis	18/136 (13.2%)	44/273 (16.1%)	28/147 (19.0%)	12/84 (14.3%)	4/42 (9.5%)
Clinical laboratory investigations					
White blood cells/nL	5.4 (4.4–6.5)	6.9 (5.5–8.3)	6.5 (5.3–7.9)	7.1 (6.0–9.1)	7.4 (6.2–8.7)
Neutrophils/nL	2.0 (1.5–2.7)	2.4 (1.8–3.0)	2.3 (1.7–3.0)	2.6 (2.0–2.9)	2.3 (1.9–2.9)
Neutrophils, %	38.0 (32.2–46.8)	36.0 (29.7–41.4)	36.0 (29.0–43.0)	35.0 (31.0–41.0)	35.0 (28.0–37.0)
Lymphocytes/nL	2.4 (2.0–2.9)	2.9 (2.2–3.4)	2.7 (2.2–3.3)	2.9 (2.4–3.6)	3.0 (2.5–3.6)
Lymphocytes, %	44.4 (39.1–52.3)	41.0 (35.0–47.2)	41.0 (36.0–48.0)	42.0 (34.0–46.0)	40.4 (34.4–47.8)
Monocytes/nL	0.5 (0.4–0.6)	0.5 (0.3–0.6)	0.4 (0.3–0.6)	0.5 (0.4–0.6)	0.5 (0.4–0.7)
Monocytes, %	9.0 (6.7–10.7)	7.0 (5.0–8.7)	7.0 (5.0–9.0)	7.0 (5.0–8.0)	7.0 (5.0–9.8)
Eosinophils/nL	0.2 (0.1–0.3)	0.7 (0.3–1.6)	0.5 (0.2–1.3)	1.2 (0.5–1.7)	1.0 (0.6–1.5)
Eosinophils, %	3.4 (2.2–5.8)	12.0 (5.0–20.0)	9.0 (3.9–18.0)	15.0 (8.6–21.0)	16.0 (7.8–22.8)
Basophils/nL	0.0 (0.0–0.1)	0.0 (0.0–0.1)	0.0 (0.0–0.1)	0.0 (0.0–0.0)	0.0 (0.0–0.1)
Basophils, %	0.9 (0.0–1.9)	0.0 (0.0–0.8)	0.0 (0.0–0.9)	0.0 (0.0–0.4)	0.0 (0–1.2)
Hemoglobin, g/dL	12.9 (11.8–14.3)	12.7 (11.7–14.1)	12.6 (11.6–13.8)	12.9 (11.6–14.2)	13.1 (12.2–14.2)

Data are presented as median (interquartile range) unless otherwise indicated.

Abbreviations: EW, eye worm positive (occult loiasis); EWMF, eye worm and microfilaria positive; INF, *Loa loa* infected; LN, *Loa loa* negative; mf, microfilaria; MF, microfilaria positive.

We therefore investigated associations between reported symptoms and protein levels, comparing symptomatic and asymptomatic LN and EW for trends and group differences.

We identified significant trend associations between 63 proteins and 7 self-reported symptom groups, including myalgia, arthralgia, random or Calabar swelling, pruritus, urticaria, neurological symptoms (paralysis, paresthesia), and nonspecific symptoms (fatigue, headaches) (Figure 2*A*, Supplementary Methods). Most proteins are markers of the immune response, including immunoglobulins (e.g., IGHG3, IGHM, immunoglobulin chains; n = 23), complement system activators (e.g., C1 subunits, C7, CFB, CFD, CFP; n = 8), and acute phase proteins (e.g., A2M, HP, SERPINA1, LYZ, TTR; n = 7). While many proteins exhibited linear trends from asymptomatic LN, symptomatic LN, and asymptomatic EW to symptomatic EW (e.g., the immunomodulating CD5L), others showed differential expression related to the presence of symptoms independent of *L. loa* positivity or were increased only in EW but not LN or MF patients. For instance, TTR, a negative acute phase protein, was consistently lower in symptomatic LN and EW than in the respective asymptomatic groups, whereas SHBG was particularly elevated in symptomatic EW but not in MF patients (Figure 2*C*, Supplementary Table 3).

Machine Learning Reveals Differences in Proteomic Patterns of Microfilarial and Occult *L. loa* Infections

Given the ongoing challenge in diagnosis of *L. loa* infections, especially in EW patients, we investigated whether the plasma proteomic signatures could differentiate LN from different *L. loa*–positive disease states (EW, EWMF, MF) using machine learning. We trained random forest classifiers to contrast LN with INF, with EW only, and with EWMF + MF combined.

We achieved a robust classification performance for distinguishing LN from INF (AUROC = 0.73) and EW individuals (AUROC = 0.73). Performance was even higher when differentiating MF + EWMF from LN (AUROC = 0.84, Figure 3*A*). IGHG4, IGHG3, and LCP1 were the most important features for identifying individuals with microfilarial infection (Figure 3*D*, top). Conversely, LCP1, IGHV3-64, and IGHM showed a greater relevance for classifying occult infections (Figure 3*D*, center). IGHG4, IGHG3, and LCP1 emerged as key features for detecting *L. loa* infections overall. Furthermore, we noted that IGHG4 and LCP1 also displayed significant correlations with the microfilariae count in the blood (0.28 and 0.21, respectively; Figure 1*E*). IGHG4, the most important feature for distinguishing LN from MF + EWMF (Figure 3*D*, bottom) achieved a classification performance of 0.81 in a single-feature model, with a decision threshold set at a $\log_2$ abundance of

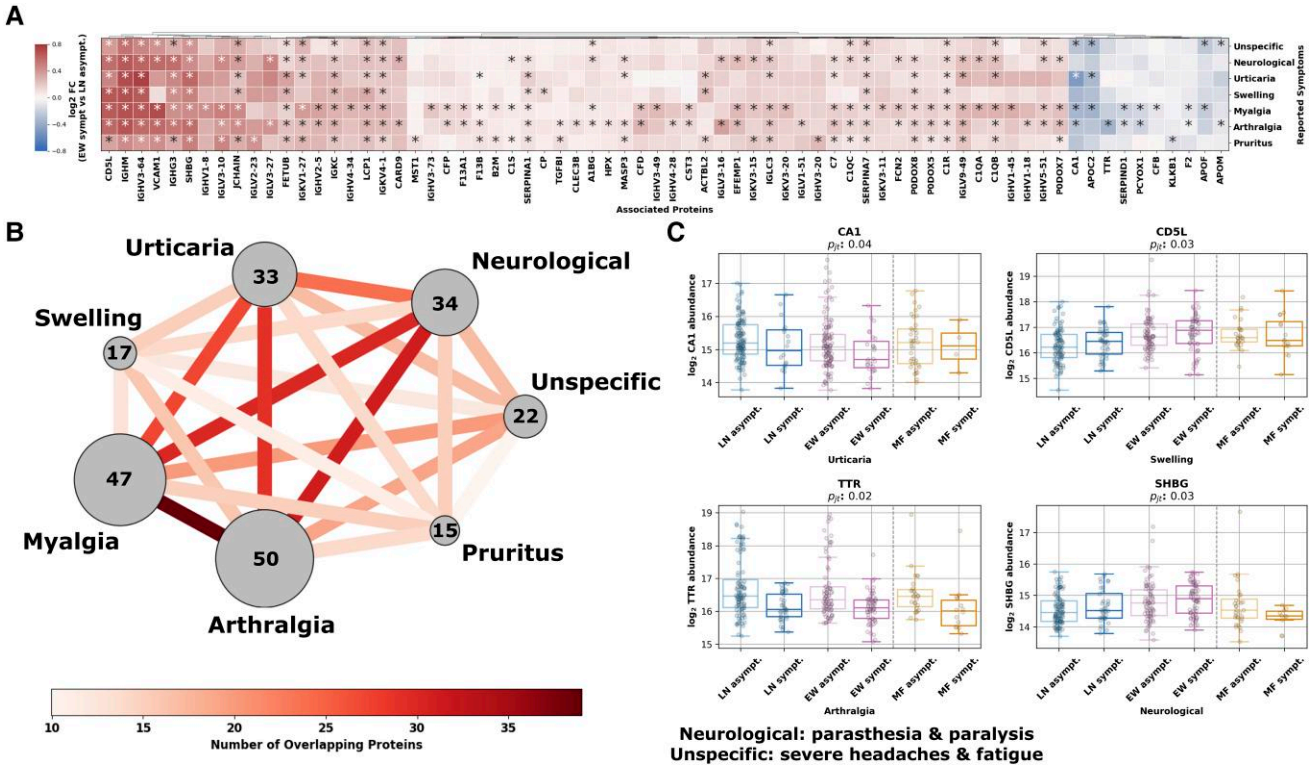

Figure 2. Comparative analysis of protein abundance trends within *Loa loa* infection symptom groups. *A*, Hierarchically clustered heatmap showing $\log_2$ fold changes in protein abundance between asymptomatic *L. loa*–negative (LN) controls and symptomatic patients with eye worm (EW) across symptom groups. Statistically significant protein trends from asymptomatic LN, symptomatic LN, asymptomatic EW, to symptomatic EW are marked with an asterisk. *B*, Network graph displaying overlap in significant protein abundance trends between symptom groups, with node size representing the number of protein associations per symptom group and edge color indicating the number of overlapping protein associations between groups. *C*, Boxplots illustrating patient groups used in trend analysis, including patients with microfilaremia for comparison; each scatter represents an individual patient sample. Abbreviations: EW, eye worm; FC, fold change; LN, *Loa loa* negative; MF, microfilaria positive; p_{jt}, *p*-value for Jonckheere-Terpstra test; SHBG, sex hormone–binding globulin; TTR, transthyretin.

19.47. Age and sex demographics of compared groups and model parameters are shown in Table 4 and 6, respectively.

Finally, we investigated the discriminatory power of our machine learning model for different microfilaria count thresholds. By setting a balanced decision threshold (predicted probability = 0.5; Figure 3*B* and 3*C*), we achieved a sensitivity of 71% when microfilarial load was <1000 mf/mL. Sensitivity increased to 79% for patients with a microfilaria count of 1000–7999 mf/mL and correctly identified all cases with microfilaria counts ≥8000 mf/mL (Supplementary Table 7).

DISCUSSION

Historically, *L. loa* infection has been viewed as a disease of limited clinical significance, usually manifesting as asymptomatic infection. More recently, there has been a shift in this perception as research has demonstrated a substantial health burden posed by this parasite [2, 6, 7]. Loiasis is currently not considered an NTD by WHO; thus, available funding and resources are sparse. As a result, the molecular characterization of the disease has been limited so far, despite major challenges in its management. To address this gap, we generated a comprehensive dataset and provide a high-resolution analysis of the highly abundant and physiologically critical fraction of the plasma proteome of 274 *L. loa*–infected individuals and 136 *L. loa*–negative controls from a hyperendemic area in Gabon. Our findings deepen the understanding of host–pathogen interactions in loiasis, with potential implications for both research and patient care.

It was recently found that the different infection states of loiasis may differ with regard to subjective symptom occurrence, eosinophilia, and *L. loa*–specific immunoglobulin levels [8, 12]. Here, we found distinct proteomic signatures of the host that differentiated between infected and noninfected individuals as well as between these different disease states. Interestingly, there were no differences of protein abundance between EWMF and MF patients, indicating that the presence of microfilaria overall dominates the plasma proteomic host response. We further observed an increasing trend of protein abundance from LN to EW to EWMF/MF for 4 proteins, and the abundance of all these proteins correlated with microfilaria count (Figure 1*C* and 1*E*). The continuum of these 4 proteins, which were overall the markers with the most significant difference in abundance compared

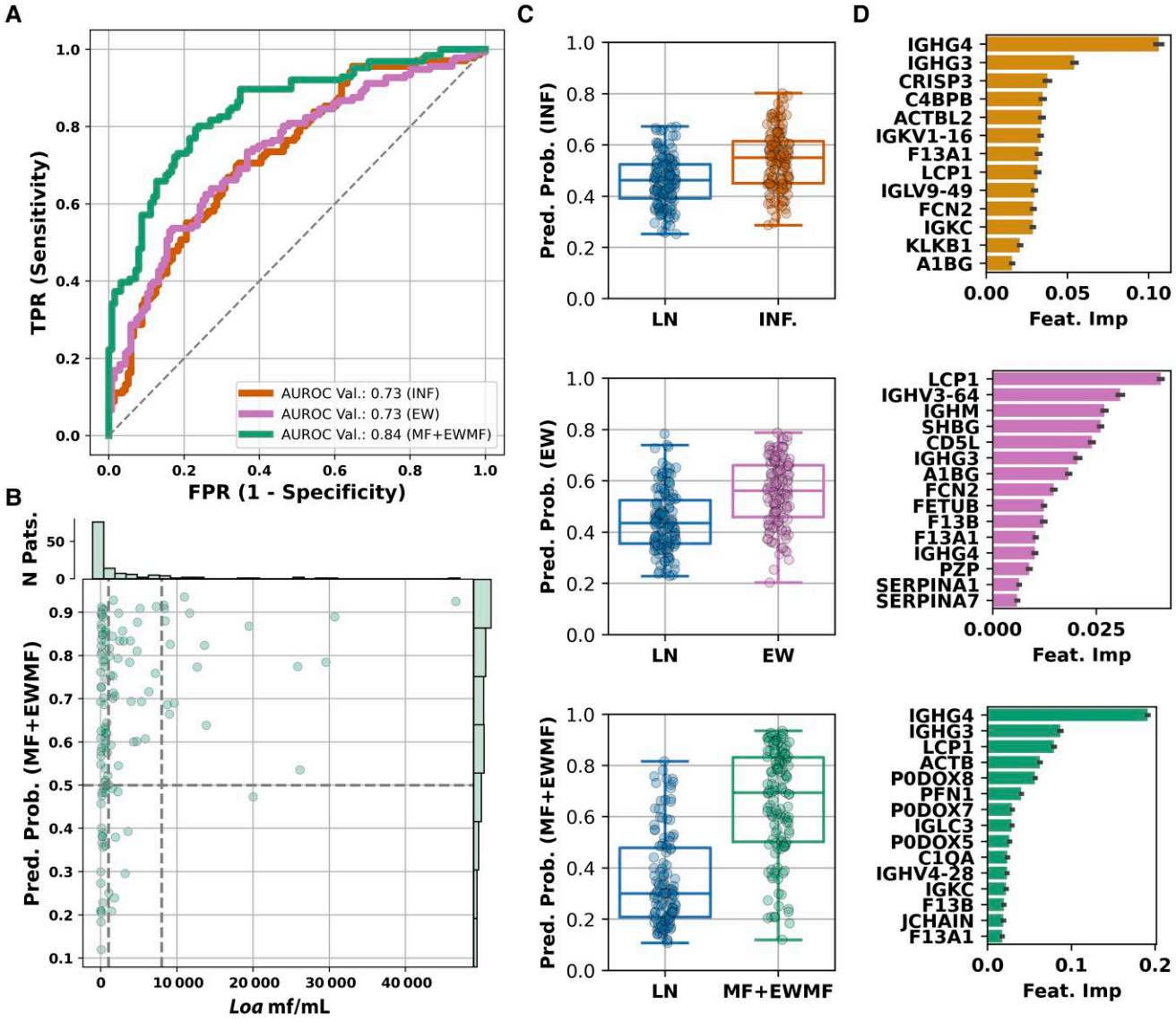

Figure 3. Machine learning (ML) classifier performance and feature importance in differentiating *Loa loa* infection states. *A*, Receiver operating characteristic curves illustrate the performance of the ML classifier, comparing *L. loa*–negative to all *L. loa*–infected cases (orange), eye worm (pink), and microfilaria positive (MF + eye worm and microfilaria positive [EWMF]; green). The color scheme remains consistent across all panels. *B*, Scatterplot showing *L. loa* microfilaria count vs the predicted probability of MF + EWMF as determined by the ML model. Histograms show patient (x-axis) and predicted probability (y-axis) distribution. Vertical dashed lines mark microfilaria count thresholds of 1000 and 7999 mf/mL. *C*, Boxplots showing predicted probabilities of the trained random forest ML models. Decision threshold for all models was fixed at 0.5 to favor neither sensitivity nor specificity. Each scatter represents 1 patient in the test set. *D*, Fifteen most important features identified by the random forest ML models (colors correspond to *A*). Abbreviations: ML, Machine Learning; AUROC, area under the receiver operating characteristic curve; EW, eye worm positive; EWMF, eye worm and microfilaria positive; Feat. Imp, feature importance; FPR, false positive rate; INF, *Loa loa* infected; LN, *Loa loa* negative; mf, microfilariae; MF, microfilaria positive; N Pats., number of patients; Pred. Prob., predicted probability; TPR, true positive rate.

to LN, thus portrays occult loiasis as a milder form of infection rather than a completely distinct entity and could potentially inform disease classification and patient stratification in future studies. However, we also found 2 proteins with specifically increased abundance in EW patients.

Importantly, our analysis identified symptom-dependent proteomic signatures. Numerous markers of the immune response exhibited linear trends from asymptomatic LN to symptomatic LN, asymptomatic EW, and symptomatic EW patients. Particularly TTR, a negative acute phase protein, was consistently lower across symptomatic individuals, whereas SHBG was notably elevated in symptomatic EW but not in MF patients. These findings underline the special nature of occult loiasis, which is associated with the highest symptom load, but has clinically been largely neglected so far.

Compared to other infectious diseases such as coronavirus disease 2019, mpox, or malaria, alterations of the plasma proteome in *L. loa* infection were less pronounced [15, 16, 27, 28].

This is unsurprising from a parasitological point of view, as *L. loa* strives to sustain chronic infections where filarial immune modulation allows long-term survival in the host. Consequently, our machine learning classifier performed moderately (AUROC = 0.73) when distinguishing LN from EW patients. However, when separating LN from patients with microfilaremia, we achieved a robust classification (AUROC = 0.84). The proteins most contributing to these classifications closely align with findings from the differential abundance analysis, with LCP1, IGHG3, and IGHG4 among the most frequently selected features, and ACTB(L2) only in the presence of microfilariae. Increased levels of IGHG4, IGHG3, ACTBL2, and LCP1 in *L. loa*–infected patients were confirmed in additional targeted hrMRM measurements. Interestingly, elevated levels of IgG4 (IGHG4) have previously been linked to parasitic infections and were shown to interact with anti-parasitic immunoglobulin E in other nematode diseases [29, 30], dampening immune responses [31]. In contrast, an increase in IgG3 (IGHG3) would indicate a more vigorous immune response and may even suggest some degree of immunity [32]. Besides these immunoglobulins, elevated ACTB and LCP1, both involved in actin metabolism, may result from actin release into the bloodstream due to phagocytosis and tissue remodeling. The interplay of these 4 proteins highlights the complexity of the human host's response to filarial, specifically *L. loa*, infections. Interestingly, we noted a distinctly modulated response in comparison to the proteomic profile of a different filarial infection, *Wuchereria bancrofti*, which is characterized by a pronounced shift in acute phase proteins [33].

With the focus on high-abundant plasma proteins that reflect the human metabolic and physiological response to disease, our dataset is primarily suited to understand the nature of the host–pathogen interactions in loiasis. However, as these proteins can also be used for the development of clinical tests, our study reveals a potential for patient management. For example, there is a substantial need to develop fast, inexpensive, and easy-to-use tools to identify patients with hypermicrofilaremia, as they are at risk to develop serious adverse events when treated with ivermectin, a situation still hampering the elimination of onchocerciasis in coendemic regions. Greene et al. recently demonstrated that an MS-based antigen assay, designed around the *L. loa*–specific Ll-Bhp-1 peptide, can effectively detect microfilarial infections (sensitivity >80%) in cases with higher parasite loads (>8000 mf/mL) [34]. However, sensitivity decreases in patients with lower parasite counts. Our machine learning classifier identified all 19 cases with ≥8000 mf/mL blood and maintained a moderate sensitivity (71%–79%) in individuals with lower counts. Notably, these results are based on the overall host proteome response, suggesting that sensitivity could be further increased with an assay that focuses on specifically selected peptides.

It is currently unknown why *L. loa* infection remains occult in some individuals, while others develop (hyper-)microfilaremia. Microfilaremia and especially hypermicrofilaremia are increasingly understood to be associated with a significant risk for long-term complications, including kidney damage, neurological impairment, and excess mortality [7]. Our analysis identified several proteins that correlated with microfilariae count, again most strongly with IGHG4. These findings support immunological mechanisms as relevant underlying factors for organ impairment and long-term complications in loiasis, highlighting an urgent need for further studies to assess the impact of chronic filarial infections on the human host.

Our study has several limitations. First, confounding of *L. loa*–specific proteomic signatures by other coendemic pathogens cannot be ruled out. To mitigate this risk, all patients with *Mansonella* spp. or *Plasmodium* spp. coinfections were excluded from the analysis, as were negative controls with eosinophilia possibly indicative of undetected helminth infections. Furthermore, definitive diagnosis of previous eye worm episodes remains difficult, as the currently best available tool, the RAPLOA questionnaire, depends on patients' self-reported symptoms and may be subject to bias.

In summary, we present the first large-scale plasma proteomics analysis of individuals living in *L. loa*–endemic regions using LC-MS/MS proteomics, quantifying the physiologically important high-abundant fraction of the plasma proteome and providing novel insights into this poorly understood neglected infectious disease. We found several markers responding to *L. loa* infection compared to negative controls and demonstrated a different host response depending on infection states. Our data underline a thus far underestimated complexity of the disease and might pave the way for improved diagnostic and disease management tools for loiasis in the future.

Supplementary Data

Supplementary materials are available at *The Journal of Infectious Diseases* online (http://jid.oxfordjournals.org/). Supplementary materials consist of data provided by the author that are published to benefit the reader. The posted materials are not copyedited. The contents of all supplementary data are the sole responsibility of the authors. Questions or messages regarding errors should be addressed to the author.

Notes

Acknowledgments. We thank all participating communities and all volunteers for participation. Furthermore, we would like to thank all colleagues who helped during the survey, especially Madame Augustine Epee and Roger Brothier Mouckoga. We thank the Charité Core Facility High Throughput Mass Spectrometry and Till Ansgar Zachow, Janine Gerdes, Claudia Conrad, Cäcilie von Wedel, and Stefanie Jentzsch at the Department of Infectious Diseases and Critical Care

Medicine for sample preparation. The graphical abstract was created with Biorender.com.

Author contributions. Conceptualization and supervision: M. Ram., M. Ral., and F. K. Sample collection: L. V., D. S., and J. H. Data curation: C. D., P. T.-L., L. V., and M. M. Formal analysis: C. D., P. T.-L., and B. Z. Funding acquisition: L. V., M. Ram., M. Ral., and F. K. Investigation: Z. W., A. F., L. B., P. K., A. N., D. L., and M. M. Methodology: C. D., P. T.-L., L. V., M. Ram., M. Ral., and F. K. Software: C. D. and B. Z. Visualization: C. D., P. T.-L., M. Ral., and F. K. Writing–original draft: C. D., P. T.-L., L. V., M. Ram., M. Ral., and F. K. Writing–review and editing: All authors.

Disclaimer. The funders had no role in study design, data collection and analysis, decision to publish, or preparation of the manuscript.

Data availability. Analysis code can be accessed in GitHub at https://github.com/ClemensDie/loa_proteome. Proteomic data, FASTA files for spectral library annotation, and DIA-NN peptide/protein quantities are available via ProteomeXchange with the identifier PXD057547. The hrMRM data and a list of fragments used for quantification have been uploaded under the identifier PXD063487.

Funding. This work was supported by the Bundesministerium für Bildung, Wissenschaft und Forschung (Austria) as part of the European and Developing Countries Clinical Trials Partnership 2 (EDCTP2), which is supported by the European Union (grant number A12/B-2 to M. Ram.), the Deutsches Zentrum für Infektionsforschung (Germany) (grant number TI 07.001 to L. V.), and the Bundesministerium für Bildung und Forschung (Germany) (grant number 031L0286B to M. Ral. and F. K.).

Potential conflicts of interest. M. Ral. is founder and shareholder of Eliptica Ltd. M. M. is a consultant and shareholder of Eliptica Ltd. All other authors report no potential conflicts of interest.

All authors have submitted the ICMJE Form for Disclosure of Potential Conflicts of Interest. Conflicts that the editors consider relevant to the content of the manuscript have been disclosed.

References

1. Ramharter M, Butler J, Mombo-Ngoma G, Nordmann T, Davi SD, Zoleko Manego R. The African eye worm: current understanding of the epidemiology, clinical disease, and treatment of loiasis. Lancet Infect Dis **2024**; 24:e165–78.
2. Veletzky L, Hergeth J, Stelzl DR, et al. Burden of disease in Gabon caused by loiasis: a cross-sectional survey. Lancet Infect Dis **2020**; 20:1339–46.
3. Metzger WG, Mordmüller B. *Loa loa*—does it deserve to be neglected? Lancet Infect Dis **2014**; 14:353–7.
4. Jacobsen KH, Andress BC, Bhagwat EA, et al. A call for loiasis to be added to the WHO list of neglected tropical diseases. Lancet Infect Dis **2022**; 22:e299–302.
5. Hemilembolo MC, Niama AC, Campillo JT, et al. Excess mortality associated with loiasis: confirmation by a new retrospective cohort study conducted in the Republic of Congo. Open Forum Infect Dis **2023**; 10:ofad103.
6. Chesnais CB, Takougang I, Paguélé M, Pion SD, Boussinesq M. Excess mortality associated with loiasis: a retrospective population-based cohort study. Lancet Infect Dis **2017**; 17: 108–16.
7. Campillo JT, Hemilembolo MC, Pion SDS, et al. Association between blood Loa loa microfilarial density and proteinuria levels in a rural area of the Republic of Congo (the MorLo project): a population-based cross-sectional study. Lancet Microbe **2023**; 4:e704–10.
8. Veletzky L, Eberhardt KA, Hergeth J, et al. Distinct loiasis infection states and associated clinical and hematological manifestations in patients from Gabon. PLoS Negl Trop Dis **2022**; 16:e0010793.
9. Mischlinger J, Veletzky L, Tazemda-Kuitsouc GB, et al. Behavioural and clinical predictors for loiasis. J Glob Health **2018**; 8:010413.
10. Klion AD, Vijaykumar A, Oei T, Martin B, Nutman TB. Serum immunoglobulin G4 antibodies to the recombinant antigen, Ll-SXP-1, are highly specific for *Loa loa* infection. J Infect Dis **2003**; 187:128–33.
11. Pion SDS, Demanou M, Oudin B, Boussinesq M. Loiasis: the individual factors associated with the presence of microfilaraemia. Ann Trop Med Parasitol **2005**; 99:491–500.
12. Veletzky L, Eberhardt KA, Hergeth J, et al. Analysis of diagnostic test outcomes in a large loiasis cohort from an endemic region: serological tests are often false negative in hyper-microfilaremic infections. PLoS Negl Trop Dis **2024**; 18:e0012054.
13. Zouré HGM, Wanji S, Noma M, et al. The geographic distribution of *Loa loa* in Africa: results of large-scale implementation of the Rapid Assessment Procedure for Loiasis (RAPLOA). PLoS Negl Trop Dis **2011**; 5:e1210.
14. Takougang I, Meremikwu M, Wandji S, et al. Rapid assessment method for prevalence and intensity of *Loa loa* infection. Bull World Health Organ **2002**; 80:852–8.
15. Demichev V, Tober-Lau P, Lemke O, et al. A time-resolved proteomic and prognostic map of COVID-19. Cell Syst **2021**; 12:780–94.e7.
16. Wang Z, Tober-Lau P, Farztdinov V, et al. The human host response to monkeypox infection: a proteomic case series study. EMBO Mol Med **2022**; 14:e16643.
17. Sang H, Petithory J. Techniques de concentration des microfilaires sanguicoles. Bull Soc Pathol Exot **1963**; 56:197–206.
18. Bouyou Akotet MK, Owono-Medang M, Mawili-Mboumba DP, et al. The relationship between microfilaraemic and amicrofilaraemic loiasis involving co-infection with *Mansonella perstans* and clinical symptoms in an exposed population from Gabon. J Helminthol **2016**; 90:469–75.

19. Tarca AL, Romero R, Bhatti G, et al. Human plasma proteome during normal pregnancy. J Proteome Res **2022**; 21: 2687–702.
20. Shomali W, Gotlib J. World Health Organization–defined eosinophilic disorders: 2022 update on diagnosis, risk stratification, and management. Am J Hematol **2022**; 97:129–48.
21. Messner CB, Demichev V, Wendisch D, et al. Ultra-high-throughput clinical proteomics reveals classifiers of COVID-19 infection. Cell Syst **2020**; 11:11–24.e4.
22. Demichev V, Messner CB, Vernardis SI, Lilley KS, Ralser M. DIA-NN: neural networks and interference correction enable deep proteome coverage in high throughput. Nat Methods **2019**; 17:41–4.
23. Pedregosa F, Varoquaux G, Gramfort A, et al. Scikit-learn: machine learning in python. J Mach Learn Res **2011**; 12: 2825–30.
24. Kistner F, Grossmann JL, Sinn LR, Demichev V. QuantUMS: uncertainty minimisation enables confident quantification in proteomics. bioRxiv [Preprint]. Posted online 24 June 2023. doi.org:10.1101/2023.06.20.545604
25. Dordevic N, Dierks C, Hantikainen E, et al. Extensive modulation of the circulating blood proteome by hormonal contraceptive use across two population studies. Commun Med (Lond) **2025**; 5:131.
26. Lehallier B, Gate D, Schaum N, et al. Undulating changes in human plasma proteome profiles across the lifespan. Nat Med **2019**; 25:1843–50.
27. Kumar V, Ray S, Aggarwal S, et al. Multiplexed quantitative proteomics provides mechanistic cues for malaria severity and complexity. Commun Biol **2020**; 3:683.
28. Demichev V, Tober-Lau P, Nazarenko T, et al. A proteomic survival predictor for COVID-19 patients in intensive care. PLoS Digit Health **2022**; 1:e0000007.
29. Turner JD, Faulkner H, Kamgno J, et al. Allergen-specific IgE and IgG4 are markers of resistance and susceptibility in a human intestinal nematode infection. Microbes Infect **2005**; 7: 990–6.
30. Hagan P, Blumenthal UJ, Dunn D, Simpson AJ, Wilkins HA. Human IgE, IgG4 and resistance to reinfection with *Schistosoma haematobium*. Nature **1991**; 349:243–5.
31. Rispens T, Huijbers MG. The unique properties of IgG4 and its roles in health and disease. Nat Rev Immunol **2023**; 23:763–78.
32. Damelang T, Rogerson SJ, Kent SJ, Chung AW. Role of IgG3 in infectious diseases. Trends Immunol **2019**; 40: 197–211.
33. Kumar V, Mishra A, Yadav AK, Rathaur S, Singh A. Lymphatic filarial serum proteome profiling for identification and characterization of diagnostic biomarkers. PLoS One **2022**; 17:e0270635.
34. Greene SE, Huang Y, Fischer K, et al. A novel antigen biomarker for detection of high-level of *Loa loa* microfilaremia. PLoS Negl Trop Dis **2024**; 18:e0012461.